Airblast spray characteristics of planar liquid films in longitudinal gas-phase shear layers at various ambient pressure conditions

K. Yoshida[1], K. Ide[1], S. Takahashi[2], K. Matsuura[*3], J. Iino[4], Y. Kurosawa[3], S. Hayashi[2] and Y. Ohta[1]

1: Department of Mechanical Engineering, Waseda University, Japan
2: Department of Mechanical Engineering, Hosei University, Japan
3: Aviation Program Group, Japan Aerospace Exploration Agency, Japan
4: Advanced Science & Intelligence Research Institute Corp., Japan

keisuke-yoshida@asagi.waseda.jp and matsuura.kazuaki@jaxa.jp

Abstract

A planar filming-type airblast atomizer was developed to study the effects of longitudinal gas-phase shear strength on its spray characteristics and to obtain a better understanding on spray phenomena of practical atomizers for aero-engine applications. The shear intensity was varied by changing the angles of the guide vanes and the air passages (α) of 0, 30, 45 and 50deg. The performance of the atomizer in terms of air flow field characteristics was firstly evaluated by single-phase numerical simulations. Its spray characteristics were then investigated by the phase Doppler anemometry, at various test conditions including elevated ambient pressure cases (p_a=0.10-0.82MPa). As a result, the clear tendency on the effect of shear strength on atomization enhancement is only observed for the higher ambient pressure and the lower fuel flow rate cases. This is mainly due to the relative population increase of small droplets rather than the decrease of large ones. For the rest, the tendency is not clear. A comparison of the present results with those of the counter-swirl airblast atomizer studied by the present authors suggests the clear effects of swirl combination on the droplet sizes observed in the previous work is not primarily due to the local circumferential shear intensity near the atomizer lip but to other effects such as widely distributed vorticity field by the swirl and/or the centrifugal effects.

Introduction

Airblast atomization of fuel films is a promising concept for the reduction of smoke and NOx emissions from aero-engines because of its good air/fuel mixing performance [1]. Recently, Matsuura et al. [2] intensively investigated the effects of swirl combinations on the spray characteristics of a double-swirl filming type airblast atomizer at atmospheric pressure conditions and Yoshida et al. [3] extended the work to assess the effects of ambient pressure (p_a). For a normalized air pressure drop across the atomizer ($\Delta p/p_t$) of 4%, they showed that when changing the outer swirl vane angle (*OSA*) from +20 to +60deg with the inner swirl vane angle (*ISA*) fixed at -45deg (counter swirl combinations), the minimum *SMD* is obtained at *OSA* between +45 to +50deg. Possible explanations for this tendency would include (a) the effects of the intensity of circumferential shear, (b) weaker interaction of the liquid film with the outer swirling air for larger *OSA*, (c) the effects of deceleration of air velocity downstream by spreading of the swirling flows and so on. There are other literatures available on the effects of swirl combinations [4-6]. Among them, for example, Aigner and Wittings [4] tried to correlate atomization quality with the wall shear stress of prefilmer lips and also to explain better atomization of counter-swirl cases than co-swirl ones by more enhanced turbulence due to stronger circumferential shear. However, what is the dominant factor on atomization quality is not well identified yet.

The motivation of the present study is to obtain a clue for a better understanding of the results of Ref. [2,3] described above, by firstly focusing on the effects of shear intensity on atomization characteristics and to which degree it is important when compared with the other parameters. For this purpose, a planar airblast atomizer was developed with which the effects (b) and (c) caused by centrifugal forces are eliminated. The atomizer is, in principle, a modified version of conventional two-dimensional filming-type airblast ones which were used by numerous authors [7-12]. However, its main feature is that the two air streams sandwiching the fuel film have spanwise velocity components which are opposed to each other. They generate longitudinal shear so that such atomizer configuration can partially simulates the atomization phenomena of practical counter-swirl airblast at-

* Corresponding author: matsuura.kazuaki@jaxa.jp

omizers for aero-engines. The shear intensity was varied by changing the angle of the guide vanes in the cascades and the air flow passages. The present study is the first attempt to deal with such an issue experimentally, to the authors' knowledge. In addition to the longitudinal shear intensity, the effects of p_a, $\Delta p/p_t$, liquid flow rate (m_f) and height of the liquid passage (h) on spray characteristics were investigated, among which the effects of p_a are mainly discussed.

In this study, the gas-phase flow characteristics of the atomizer were firstly evaluated by numerical simulations during its design process. The spray characterizations were then performed experimentally by the phase Doppler anemometry (PDA). As mentioned, since to know to which degree the shear intensity affects atomization quality is our prior target, the attempt to understand detailed atomization mechanism, for example by means of close-up high-speed visualizations, is the next step and in this sense beyond the scope of this paper. Instead, the tendency on the dependence of the mean droplet sizes on the shear strength measured by the PDA is discussed here, in relation to the results of Ref. [2,3].

Planer Airblast Atomizer

The planar airblast atomizer developed for this study is shown in Fig. 1. The coordinate system used below is also defined in the figure.

The atomizer was designed so that the two air streams, having the same axial velocity but opposite spanwise velocity components to each other, meet up at the exit of the atomizer to form a longitudinal shear layer to which a planar kerosene liquid film is injected and atomized. The shear intensity was varied by changing the angle of the guide vanes in the cascades and the air flow passages (α). Totally four different shear intensity cases were investigated by changing Units A and B with α of 0, 30, 45 and 50 deg. Here, no guide vanes were equipped for α=0deg. The width of the air passages at the exit (l) is determined depending on α to satisfy the two criteria: (A) l is wider than the width of the fuel passage (40mm). (B) The width of the overlapping portion of the two air flows estimated by the simple geometrical consideration is 20mm at z=20mm (see Fig.1), again except for α =0deg. The criterion (B) ensures sufficient region of uniform spray in the spanwise direction even with dissipation effects in reality, where phenomena should be ideally two-dimensional. The values of l are shown in the table in Fig.1, together with the number of the guide vanes (N_v), and the ratios of flow coefficients of air (C) to those of potential flows with effects of α (C_0). The last were obtained by single-phase flow experiments for the cases with the Reynolds numbers based on the height of the air passages at the exit (3mm) greater than 40,000.

The liquid fuel is supplied through a fuel pipe which is connected to the cylindrical manifold. It then comes out to the planer liquid passage through ten holes whose diameters are 1mm. The liquid film is finally injected from the exit of the planer passage. Its height (h) can be varied by replacing spacer units (not shown in Fig.1), locating between Units C and D. Two height cases, h=0.2 and 0.5mm, were investigated in the present study, but the results of the latter case is mainly discussed below.

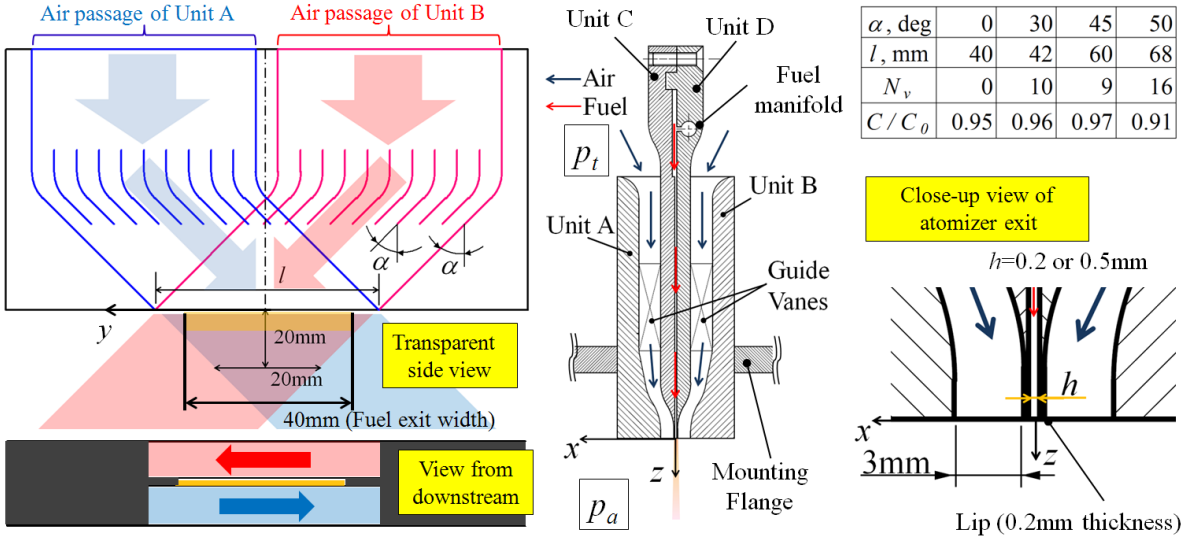

α, deg	0	30	45	50
l, mm	40	42	60	68
N_v	0	10	9	16
C/C_0	0.95	0.96	0.97	0.91

Figure 1 Schematic of planar airblast atomizer.

Experiments

Experiments were conducted by means of the high pressure spray test facility at the Japan Aerospace Exploration Agency, developed for spray experiments under elevated ambient air pressures up to about 1MPa at room temperature conditions [13].

As for test conditions, in addition to the shear intensity, several flow parameters were varied and those effects on spray characteristics were investigated, that is, the ambient pressure (p_a: 0.10, 0.23, 0.42, 0.52 and

0.82MPa), the normalized air pressure drop across the atomizer defined as the ratio of absolute pressure drop to the inlet pressure ($\Delta p/p_t$: 2, 4, 8 and 10%), and the liquid flow rate (m_f: 0.78 and 3.9g/s). The latter two conditions above correspond to the air potential velocity U_a=59, 85, 122 and 138m/s, and the bulk liquid fuel velocity (volume flow rate divided by the geometrical opening area of the fuel passage at the exit) U_f=0.05 and 0.25m/s, respectively. The discussions below focus mainly on the cases of $\Delta p/p_t$=4%.

The spray characterization was based on the phase Doppler anemometry (PDA). The measurements and post-processing were performed by a similar system and procedures described in Ref. [13], except the use of a different transmitting optics: The system consisted of a two-velocity-component DANTEC Fiber-Flow transmitter, Aerometrics PDI receiver, and Artium ASA signal processors. The PDA setup is summarized in Table 1. Though axial and spanwise droplet velocity (v_z and v_y) could be measured by the PDA, the results of the axial droplet velocity are mainly discussed below. This is because the system was not operated in the "coincidence mode [14]" for time-efficient data acquisition with the higher validation rates, so that the simultaneous size/velocity measurements were only achieved for the axial velocity component. Two different settings on the total beam power at the probe volumes were used depending on the flow operation conditions to simultaneously avoid too frequent saturation of photomultipliers and signal loss from small droplets. The effect of the difference of the power settings was examined in some test cases and it only caused 1.7μm difference of *SMD* at most.

Table 1 PDA optical setup.

Transmitter		Probe volume (PV)	
Laser	4W Ar^+ laser	Total beam power (G)	66[*3] and 144[*4] mW
Wavelength (G[*1])	514.5nm	Total beam power (B)	46[*3] and 76[*4] mW
Wavelength (B[*2])	488.0nm	Size (G)	127μm (dia.) x 1.77mm(length)
Focal length	500mm	Size (B)	121μm (dia.) x 1.68mm(length)
Beam separation at front lens	72.2mm	Slit width projected on PV	300μm
Beam diameter at front lens	2.57mm (G and B)	Fringe separation (G)	3.57μm
Receiver		Fringe separation (B)	3.39μm
Focal length	500mm	Phase-diameter conversion factor	0.217μm/deg
Effective lens diameter	72mm	[*1] For green beams	[*2] For blue beams
Scattering angle	70deg	[*3] For $\Delta p/p_t$ <8%	[*4] For $\Delta p/p_t \geq$8%

Numerical Simulation

Gas-phase numerical simulations in the absence of fuel at atmospheric conditions were performed during the design process of the atomizer. Similar to Ref. [2], we employed the UPACS (Uniform Platform for Aerospace Computational Simulation) three-dimensional compressible code developed by the Japan Aerospace Exploration Agency, based on the Reynolds-averaged Navier-Stokes Equations with the Spalart-Allmaras turbulent model. A sketch of the calculation domain for the case of α=45deg is presented in Fig.2 as a thinned-out grid view. The structured grid system consists of more than ten million grids with the smallest grid size of 0.05mm. As for the downstream region of the injector, a cylindrical region, 310.5mm in diameter and 600 mm in length, was considered to simulate the flow duct of the test facility. The protrusion of the atomizer in the downstream direction with respect to the mounting flange surface (see Fig.1) for the better optical access in the experiments was not considered in the CFD so that the flange surface is also on z=0 plane. The solid boundary condition was applied for the cylindrical wall, whereas the total pressure at the inlet of the injector and the static pressure at the exit of the cylinder were fixed through the calculation, so that the pressure drop defined between these two locations in the numerical simulations was kept at 4%.

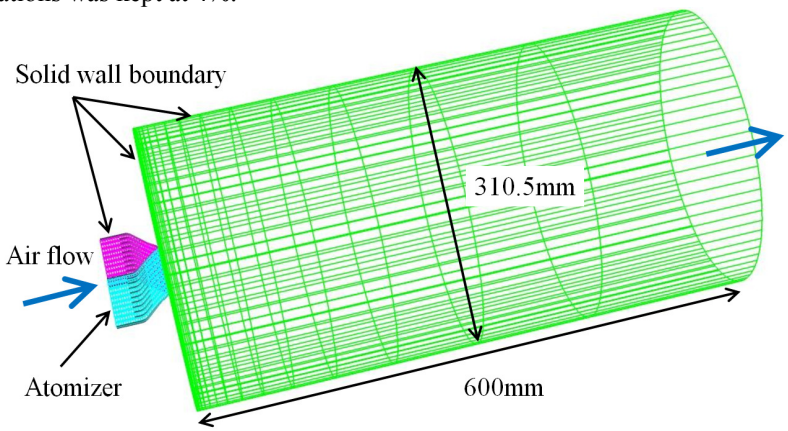

Figure 2 Sketch of numerical calculation domain for α=45deg.

Results and discussions

First of all, gas-phase velocity fields inside and downstream of the atomizer were evaluated. The mean absolute velocity (V_{abs}) obtained by CFD is presented in Fig. 3 for the single phase flows at p_a=0.10MPa and $\Delta p/p_t$ =4%. The results are those on a mesh surface designated as S_m, which is located at the middle height of the air passage of unit A for z<0 and then coincides the plane of x=1.95mm for z>0. The results show that the non-uniformity of V_{abs} in the spanwise direction at the atomizer exit due to the wakes of the guide vanes are reasonably low and are 12% of V_{abs} at most in the range of y=-0.35l~0.35l (70% of air passage width). The flow angles φ defined by φ =atan(V_y/V_z) at the exit obtained by the CFD are 24~27, 37~40, and 44~47deg for α=30, 45 and 50deg, respectively, for the same y-range above. The values of φ are lower than those of α as expected, which is mainly due to the contraction of the flow passage in x direction. The small variations of φ (within 3deg at most) are not due to the wake effects: In general, the higher φ is observed in the closer regions to the side wall (y=l/2).

Figure 4 shows the CFD results of mean axial and spanwise velocity profiles (V_z and V_y) in x direction at (y,z)=(0,0) and (0,15) for p_a=0.10MPa and $\Delta p/p_t$ =4%. In addition, the PDA results of the two corresponding droplet velocity components (v_z and v_y) for the two phase flow are also presented at (y,z)=(0,15) for p_a=0.82MPa , $\Delta p/p_t$ =4% and m_f=0.78g/s (the less mass loading case). For the latter conditions, since more than 95% of droplets were smaller than 25μm, and the droplets in this size range has only weak dependence of mean axial velocity on their size (less than 2m/s difference) for x=-4~4mm, the mean slip velocity would be almost negligible in the shear layer of interest. Thus, neglecting Reynolds number effects for mean gas velocity field, the droplet velocity should give reasonable estimate for air velocity. However in fact, the discrepancy is observed between the two results, so that the gas-phase velocity field measurement is required for a better comparison. Nevertheless, general tendency is in common, for example, obviously the stronger longitudinal shear is obtained for the larger α. In this sense, the air flow field of the atomizer is as expected and is suitable for the present purpose.

Secondly, some preliminary spray evaluation was preformed. Typical spray photographs are presented in Fig. 5 for $\Delta p/p_t$ =4%, α=0 and 45deg. In general, the whole span of the fuel exit is less likely to be filled up by fuel for the lower m_f cases and/or the higher p_a cases. This is similar to what Bhayaraju [10] pointed out for their non-prefilming type atomizer. For m_f=3.9g/s, it looks almost filled up but the images with 1ms exposure show

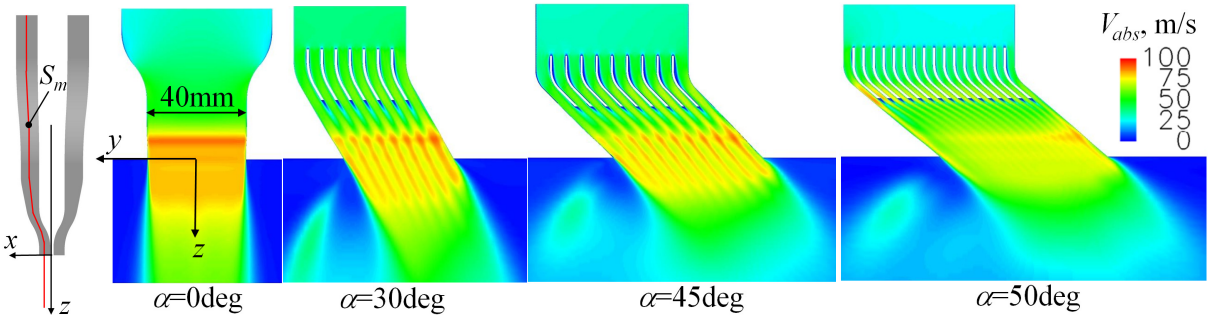

Figure 3 Mean absolute velocity contours by CFD on surface S_m (p_a=0.10MPa, $\Delta p/p$=4%, h=0.5mm).

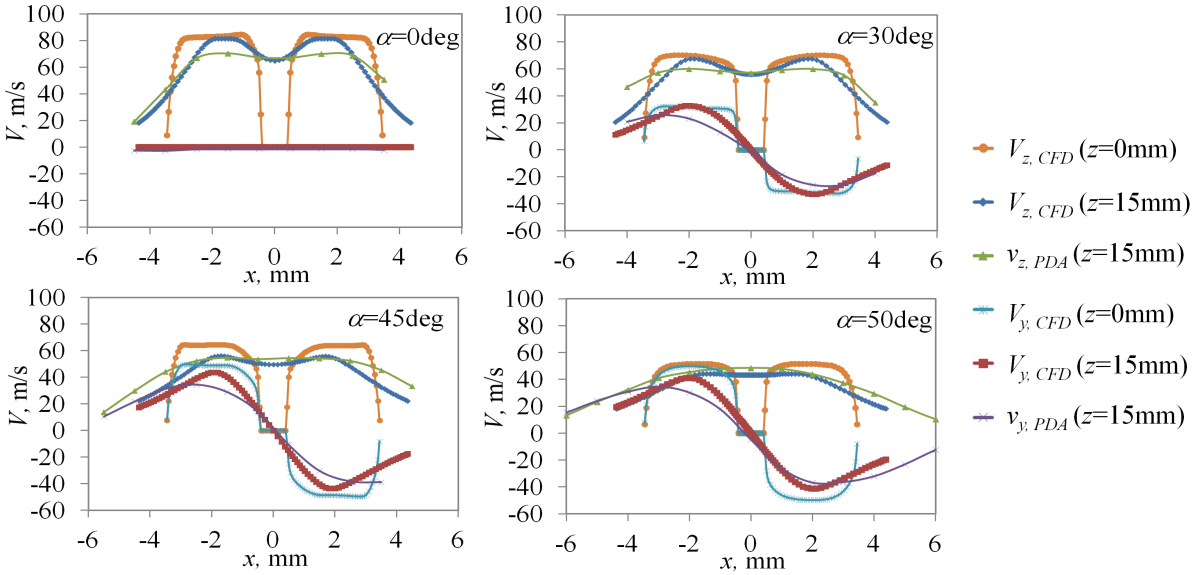

Figure 4 Mean velocity profiles of air by CFD and those of droplets by PDA in x directions (CFD: p_a=0.10MPa, $\Delta p/p$=4%, h=0.5mm, PDA: p_a=0.82MPa, $\Delta p/p$=4%, m_f=0.78g/s, h=0.5mm).

non-uniform and periodical-like structures in the spanwise direction. The structure for α=45deg looks rather relevant to the number of the vanes in contrast to the case of α=0deg in which such pattern seems in relation to fluid-dynamic instability. The image of Fig5-h is instinctively similar to the left figure in Fig.1.

Typical PDA results on evaluation of the spanwise uniformity for α=30 and 45deg in terms of mean droplet axial velocity and Sauter mean diameter (*SMD*) are shown in Fig. 6. The measurement locations are at z=15mm and x=0mm, which is 5mm upstream of the location considered in the design process (z=20mm, see Fig.1). They show the spray can be regarded as almost uniform near the central region on time-average basis, at least in the range of y=-10~10mm. Therefore, the discussions below will focus on the data on the central plane (y=0), as they are considered to represent phenomena which would occur in ideal two-dimensional configurations.

Spatial distribution of the mass flux measured by the PDA data for $\Delta p/p_t$ =4% at z=15mm in x direction is presented in Fig. 7. Even for the cases of such low fuel flow rates (m_f <~5g/s), some of the presented values were affected by the poor PDA validation rate due to multiple scattering and a care is needed to interpret the data. This tendency is more pronounced for the optically denser spray cases, that is, for the higher p_a and higher m_f, and also near the central regions (x~0). Nevertheless, the results of the outer regions of the sprays where they are relatively dilute indicate that the "relative" width of the mass flux curves (or qualitatively "the spray width") of the higher shear cases to the lower shear cases generally becomes wider for the higher p_a.

Spatial distribution of 15% and 85% volume undersize diameters (d_{15} and d_{85}) in x direction is presented in Fig. 8 for the same test conditions and measurement locations. By looking through the figures from left to right, it is observed that the two diameters decrease as p_a increases. For m_f=0.78g/s, it is difficult to find consistent tendency on the effects of the shear strength on d_{15} and d_{85} for the lower ambient pressure cases (0.10 and 0.23MPa), though d_{85} in the central region is generally large for α=50deg and small for α=0deg. On the other hand, for the higher ambient pressure cases (0.42 and 0.82MPa), the measured d_{15} in the central region is smaller for the higher shear cases (α=45 and 50deg) than for the lower shear cases (α=0 and 30deg). However, such tendency is not observed for d_{85}: Especially for α=0deg, it is still relatively small compared with the other α. For m_f =3.9g/s, the tendency on d_{85} is similar to that for m_f=0.78g/s, but that on d_{15} is not observed.

Spatial distribution of mean axial velocity (v_z) and its root mean square value ($v_{z,\,rms}$) for small droplets (0-5 μm) in x direction is presented in Fig. 9 for m_f=0.78g/s. These small droplets reasonably represent gas-phase flow characters. It is found that v_z is faster for the higher p_a regardless of α. On the other hand, $v_{z,\,rms}$ increases as p_a increases for the higher shear cases, but this is not observed for the lower shear cases. For m_f=3.9g/s (not shown here), the degree of increase of $v_{z,\,rms}$ with respect to p_a is also larger for the higher shear cases.

The effects of α and p_a on global *SMD*, d_{15} and d_{85} on z=15mm cross-sectional plane are presented in Fig. 10. They were calculated by assuming spanwise uniformity and considering the weight of the number flux for each

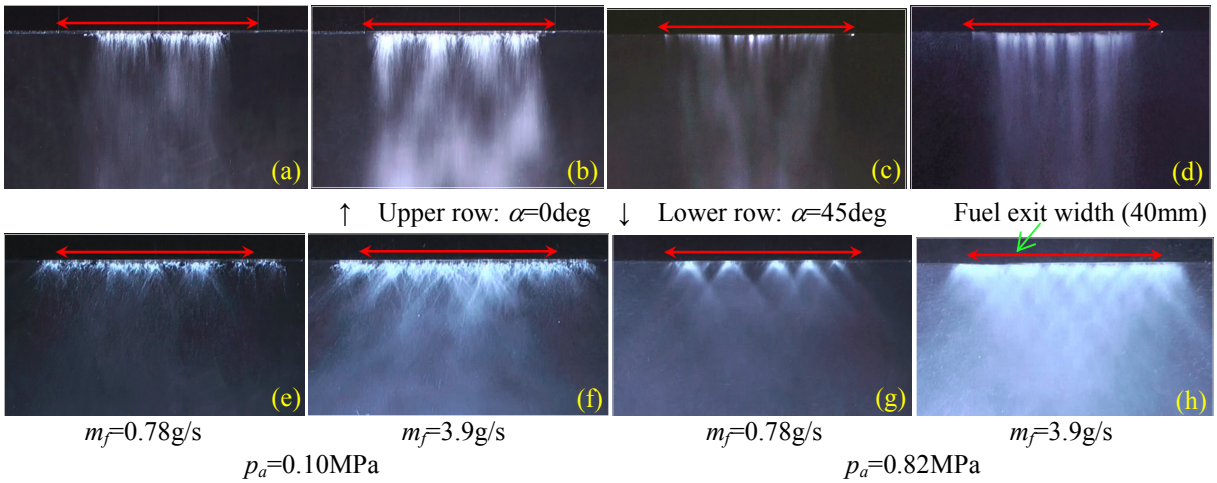

Figure 5 Typical spray images for α=0 and 45deg ($\Delta p/p$=4%, h=0.5mm, exposure time: 1ms).

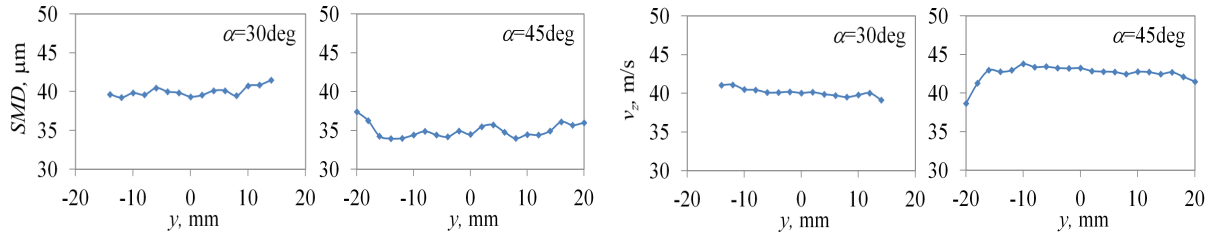

Figure 6 Spanwise variation of mean droplet axial velocity and *SMD* (α=30 and 45deg, p_a=0.10MPa, $\Delta p/p$=4%, m_f=0.78g/s, z=15mm, x=0mm, h=0.5mm).

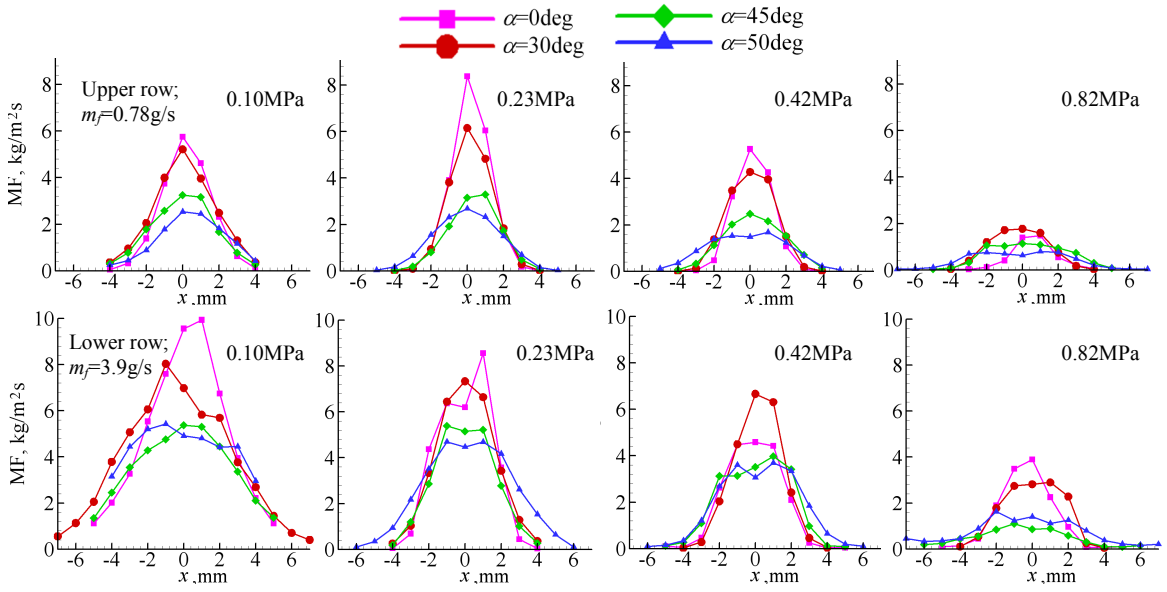

Figure 7 Distribution of mass flux in x direction ($\Delta p/p$=4%, z=15mm, y=0mm, h=0.5mm).

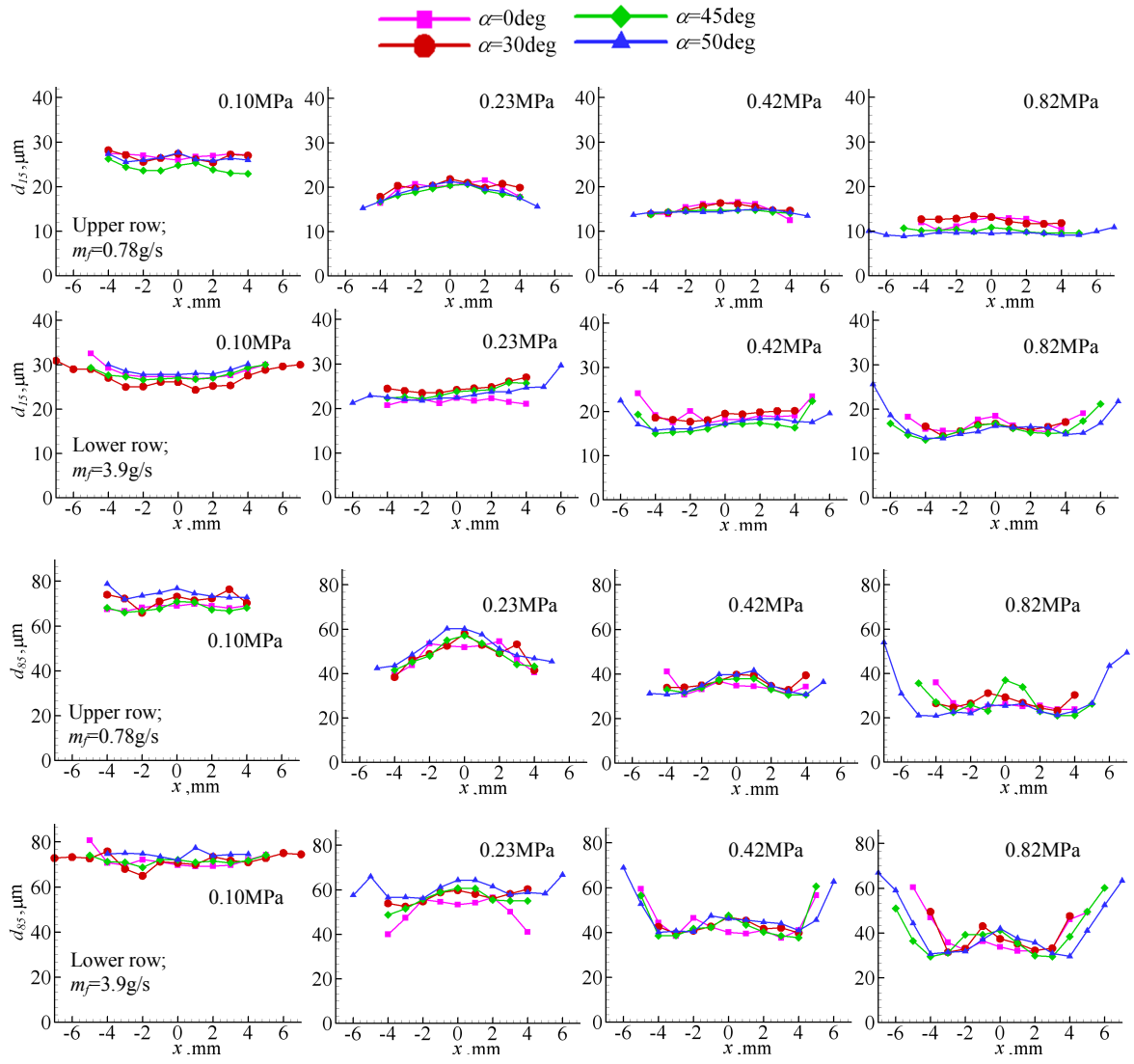

Figure 8 Distribution of 15% and 85% volume undersize diameter in x direction ($\Delta p/p$=4%, z=15mm, y=0mm, h=0.5mm).

location. There are two items interpreted from the figure, which were already mentioned in the discussion of Fig.8: (A) For m_f=0.78g/s, *SMD* is smaller for the higher shear cases in the higher p_a range. This tendency is similar to that of d_{15} rather than of d_{85}, suggesting that this is due to the contribution of relatively small droplets. On the other hand, such noticeable tendency is neither observed nor clear for m_f=3.9g/s. (B) d_{85} for the highest shear case (α=50deg) is larger than the lowest counterpart (α=0deg) at least in the lower p_a range. This tendency seems also true even in the higher p_a range for m_f=3.9g/s, though again less clear.

An explanation for the better atomization for the higher shear cases in the higher p_a range for m_f=0.78g/s would be related to the effects of turbulence transport, since higher velocity fluctuations and wider spray dispersion are observed for such cases as mentioned. On the other hand, no distinctive difference observed in d_{85} among the cases of α=0, 45 and 50deg for m_f=0.78g/s apparently seems to contradict this explanation. Better dispersion for the higher shear cases might result in less coalescence even in highly dense spray for the higher p_a , whose effects should be more evident on d_{15} than d_{85} because of relatively higher population of small droplets. Another explanation would be the difference of near-field spray structures that depend on the degree to which the fuel exit is filled up by fuel in the spanwise direction, as more evident discrete structure in Fig.5-g than in Fig.5-c, for example, would cause more efficient air entrainment. The fact that the tendency above is not as clear for m_f=3.9g/s as that for m_f=0.78g/s would support this explanation, where the fuel exit is filled up to a better extent. However, further detailed study is definitely required to clarify the main reason. The effect of the quality of the PDA signals in such dense sprays on sizing errors should be also a concern. However, this is not probably the main reason as the degree of the *SMD* difference in discussion (3μm) is beyond the effects of signal quality or repeatability, the degree of which could be estimated from those of the laser power mentioned above (1.7 μm).

On the other hand, a clearer and more important conclusion derived from the present experiments is that, comparing the present results with those of the counter-swirl airblast atomizer in Ref [2,3], the effects of swirl combination on the droplet size observed in the literatures are not primarily due to the maximum local circumferential shear intensity near the atomizer lip but other effects such as widely distributed vorticity field by the swirl and/or the centrifugal effects as pointed out in the introduction above, at least in the lower p_a range.

The plot of *SMD/h* against Weber number defined by $We = \rho U_a^2 h/\sigma$ was shown in Fig.11, including the results of the other $\Delta p/p_t$ cases than 4%. Since h and σ are constant, this actually shows the relationship between

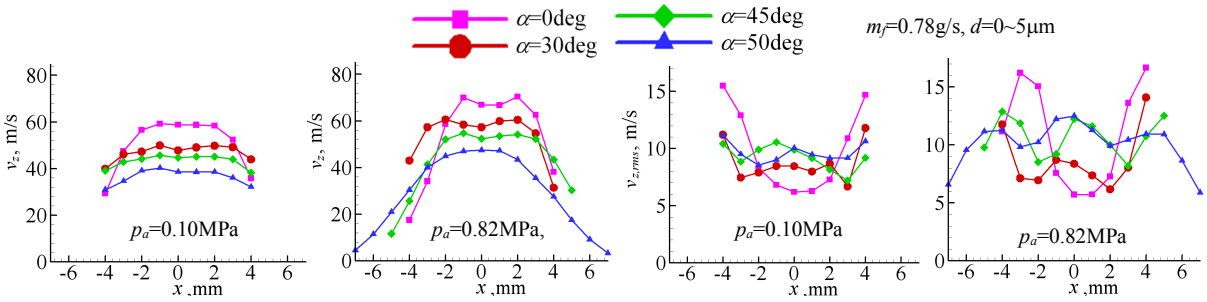

Figure 9 Distribution of mean axial velocity and its root mean square for small droplets (0-5 μm) in x direction ($\Delta p/p$=4%, m_f=0.78g/s, z=15mm, y=0mm, h=0.5mm).

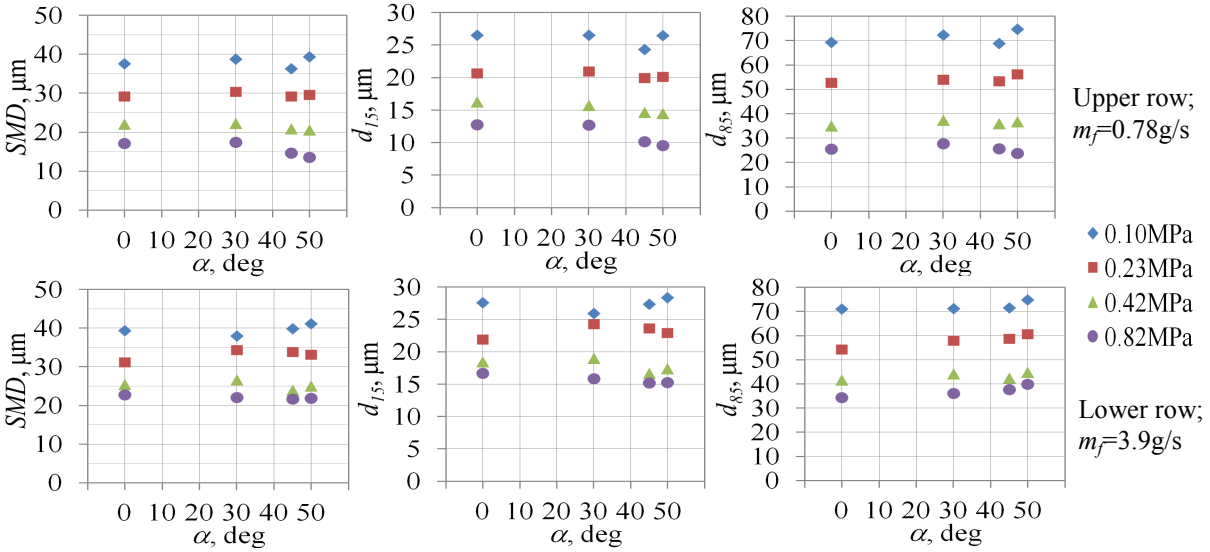

Figure 10 Effects of shear strength and ambient pressures on global *SMD*, 15% and 85% volume undersize diameters ($\Delta p/p$=4%, z=15mm, y=0mm, h=0.5mm).

the global S*MD* and air momentum flux ρU_a^2. For each α, they are well correlated, suggesting that the effects of p_a and $\Delta p/p_t$ can be primarily explained through the single parameter, ρU_a^2. This is because (A) *We* including ρU_a^2 term is a key parameter for atomization and (B) the air to fuel momentum ratio including ρU_a^2 is a key parameter for the degree to which the fuel passage is filled up [10] and thus affects the near-field spray structures.

Finally, the effect of the height (h) of the fuel passage on global *SMD* is presented in Fig. 12 for $\Delta p/p$=4% and m_f=0.78g/s. The difference between the two cases with h =0.2 and 0.5mm is small. In the present case, the lip thickness (0.2mm) is of the similar order to h, so the wake phenomena behind the lips [4] should be also considered in addition to the effects of the film thickness itself.

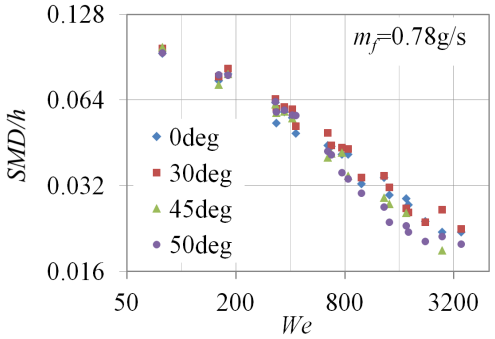

Figure 11 Dependence of normalized global *SMD* on Weber number (z=15mm, y=0mm, h=0.5mm).

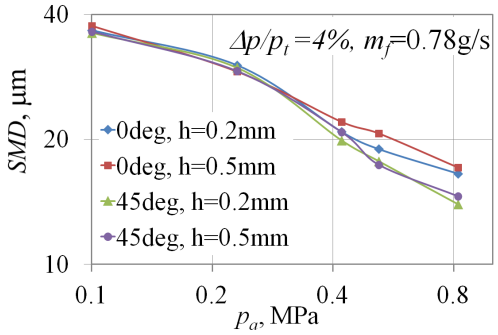

Figure 12 Dependence of global *SMD* on height of fuel passage ($\Delta p/p$=4%, m_f=0.78g/s, z=15mm, y=0mm).

Conclusions

A planar filming-type airblast atomizer was developed to study the effects of longitudinal gas-phase shear strength on its spray characteristics and to obtain a better understanding on spray phenomena of practical atomizers for aero-engine applications. The shear intensity was varied by changing the angles of the guide vanes and the air passages (α) of 0, 30, 45 and 50deg. The performance of the atomizer in terms of air flow field characteristics was firstly examined by single-phase numerical simulations and the atomizer was proven to be working almost as expected. Its spray characteristics were then investigated by means of the phase Doppler anemometry at test conditions of the ambient pressure (p_a=0.10~0.82MPa), the normalized air pressure drop across the atomizer ($\Delta p/p_t$=2~10%), the fuel flow rate (m_f=0.78 and 3.9g/s) and the height of the fuel flow passage (h=0.2 and 0.5mm). The results for $\Delta p/p_t$=4% and h=0.5mm were mainly discussed in the present paper. As a result, the clear tendency on the effect of shear strength on atomization enhancement is only observed for the higher p_a and the lower m_f cases. This is mainly due to the relative population increase of small droplets rather than the decrease of large ones. For the rest, the tendency is not clear. A comparison of the present results with those of the counter-swirl airblast atomizer studied in Ref. [2,3] suggests the clear effects of swirl combination on atomization observed in these references is not primarily due to the local circumferential shear intensity near the atomizer lip but to other effects such as widely distributed vorticity field by the swirl and/or the centrifugal effects.

References

[1] Lefebvre, A. H., *Progress in Energy and Combustion Science* 6: 233-261 (1980).
[2] Matsuura, K., Suzuki, S., Suda, M., Iino, J. and Hayashi, S., *Proceedings of 22th Annual Conference on Liquid Atomization and Spray Systems-Europe (ILASS-Europe)*, Paper No. ILASS08-1-4 (2008).
[3] Yoshida, K., Suzuki, K., Matsuura, K., Kurosawa, Y., Hayashi, S. and Ohta, Y., *Proceedings of 24th Annual Conference on Liquid Atomization and Spray Systems-Europe (ILASS-Europe)* (2011).
[4] Aigner M., and Wittig, S., *ASME 87-GT-204* (1987).
[5] Miyamoto, S., Mikami, M., Kojima, N., Fujii, A. and Saito, T., *Proceedings of 10th International Conference on Liquid Atomization and Spray Systems* (*ICLASS 2006*), Paper No. 06-133 (2006).
[6] Saitou,T. and Fujimori, *Proceedings of International Gas Turbine Congress(IGTC 99)* : 753-758 (1999).
[7] Rizk, N. K. and Lefebvre, A. H., *Journal of Engineering for Power* 1-2: 706-710 (1980).
[8] Arai, T. and Hashimoto, H., *Bulletin of JSME* 28-245: 2652-2659 (1985).
[9] Bhayaraju, U. and Hassa, C., *Atomization and Sprays*, 19-12:1147-1169 (2009).
[10] Bhayaraju, U., *Doctoral Dissertation, Technical University of Darmstadt* (2007).
[11] Fernandez, V. G., Lavergne G. and Berthoumieu, P., *Atomization and Sprays*, 21-1:1-16 (2011).
[12] Stapper, B. E., Sowa, W. A. and Samuelsen, G. S., *Journal of Engineering for Gas Turbines and Power* 114-1: 39-45 (1992).
[13] Matsuura, K., Suzuki K. and Kurosawa, Y., *Proceedings of 22th Annual Conference on Liquid Atomization and Spray Systems-Europe (ILASS-Europe)*, Paper No. ILASS08-P-4 (2008).
[14] Albrecht, H.-E., Damaschke,N., Borys, M. and Tropea, C., *Laser Doppler and phase Doppler measurement techniques,* Springer (2003).